Proc. Natl. Acad. Sci. USA
Vol. 96, pp. 9622–9627, August 1999
Cell Biology

The direction of transport through the nuclear pore can be inverted

MAXENCE V. NACHURY AND KARSTEN WEIS*

Department of Molecular and Cell Biology, University of California, Berkeley, CA 94729-3200

Communicated by Randy Schekman, University of California, Berkeley, CA, June 25, 1999 (received for review May 2, 1999)

ABSTRACT **Transport of macromolecules across the nuclear envelope is an active process that depends on soluble factors including the GTPase Ran. Ran-GTP is predominantly located in the nucleus and has been shown to regulate cargo binding and release of import and export receptors in their respective target compartments. Recently, it was shown that transport of receptor–cargo complexes across the nuclear pore complex (NPC) does not depend on GTP-hydrolysis by Ran; however, the mechanism of translocation is still poorly understood. Here, we show that the direction of transport through the NPC can be inverted in the presence of high concentrations of cytoplasmic Ran-GTP. Under these conditions, two different classes of export cargoes are transported into the nucleus in the absence of GTP hydrolysis. The inverted transport is very rapid and can be blocked by known inhibitors of nuclear protein export. These results suggest that the NPC functions as a facilitated transport channel, allowing the selective translocation of receptor–cargo complexes. We conclude that the directionality of nucleocytoplasmic transport is determined mainly by the compartmentalized distribution of Ran-GTP.**

Macromolecular transport between the nucleus and the cytoplasm occurs through the nuclear pore complex (NPC; ref. 1). The NPC contains an aqueous channel allowing passive diffusion of molecules smaller than 60 kDa in size. However, the proper localization and accumulation of most proteins and RNAs in their respective target compartments are the results of active, receptor-mediated processes.

Almost all nuclear transport events that have been characterized thus far require at least one member of the importin β (or karyopherin β) superfamily of transport receptors and the small GTPase Ran (2–4). Ran, which is predominantly located in the nucleus, is controlled both by a nuclear, chromatin-associated, guanine-nucleotide exchange factor, RCC1 (5), and by a cytoplasmic GTPase activating protein, Ran-GAP (6). The compartmentalized distribution of these two regulatory proteins predicts that nuclear Ran is predominantly loaded with GTP, whereas cytoplasmic Ran is immediately converted into the GDP-bound state. Interestingly, it was shown that import receptors (or importins) of the importin β family bind to their cargoes in the absence of Ran but release their substrates after binding to Ran-GTP (7, 8). For example, importin β binds to its cargo, the importin-α·nuclear-localization signal (NLS) protein complex, in the cytoplasm. After translocation into the nucleus, Ran-GTP induces the dissociation of the transport substrate from importin β. In contrast, export receptors (or exportins) have a high affinity for their cargoes only in the presence of Ran-GTP and release them in the cytoplasm after stimulation of GTP hydrolysis by the concerted action of RanGAP and RanBP1 (9–13). For example, proteins containing a leucine-rich nuclear export signal (NES) are exported from the nucleus via binding to exportin1/CRM1·Ran-GTP (9, 14), and importin α is transported out of the nucleus in a complex with CAS and Ran-GTP (10). These data support a model in which a Ran-GTP gradient across the NPC confers directionality in nucleocytoplasmic transport processes (8, 15–18). Although molecular interactions between importin β family members and components of the NPC have been shown, the mechanism of translocation of the receptor–cargo complexes across the NPC has remained elusive (2–4).

Here, we show that the directionality of nuclear transport can be inverted *in vitro* by cytoplasmic addition of RanQ69L-GTP. CRM1-dependent NES- as well as CAS-dependent importin α transport into nuclei could be observed under these conditions. These observations suggest that the nuclear pore is a bidirectional channel allowing facilitated transport of importin β-like factors and that the asymmetry of nucleocytoplasmic transport is mainly determined by the compartmentalized distribution of Ran-GTP.

METHODS

Recombinant Protein Expression and Protein Conjugation. Importin-α/hSRP1α, importin-β/p97, importin-β^{71-876}, CAS, Ran, ZZ-Ran, ZZ-RanQ69L, and the fusion of the importin-β-binding domain of importin-α (IBB) to β-galactosidase (βGal) were all expressed as N-terminal fusions to a His_6 tag and purified by metal-affinity chromatography on Ni^{2+}-nitrilotriacetic acid agarose (Qiagen, Chatsworth, CA) as described (19, 20).

Human CRM1 (a gift from L. Englmeier and I. W. Mattaj, European Molecular Biology Laboratory, Heidelberg) was expressed without any tag in *Escherichia coli* and purified as described (21). Untagged RanQ69L also was expressed in *E. coli* and purified as described (16).

Fluorescein labeled BSA-NES, BSA-NLS, and IBB-βGal were prepared as described (19, 22).

***In Vitro* Transport Assays.** Cells were permeabilized according to a protocol modified from refs. 19 and 23. In short, HeLa cells were grown on coverslips and permeabilized with 50 μg/ml digitonin (Fluka) in the presence of an energy-regeneration system (19) for 5 min at room temperature. The use of an energy-regeneration system during the permeabilization together with the incubation at room temperature significantly enhanced the loss of importin-β-like transport factors (i.e., CAS, importin-β, and CRM1; M.V.N. and K.W., unpublished observations). Cells were kept on ice until the reaction was started by addition of 10 μl of reaction mix onto the coverslip. His_6-ZZ-Ran and His_6-ZZ-RanQ69L were used for all experiments (except the ones presented in Fig. 3, in which His_6-Ran and untagged RanQ69L were used). Samples were visualized on a Leica (Deerfield, IL) DMR inverted microscope with a 65×/1.32 oil PLAN APO objective and then scanned with a Leica TCS NT confocal workstation. Note that

The publication costs of this article were defrayed in part by page charge payment. This article must therefore be hereby marked "*advertisement*" in accordance with 18 U.S.C. §1734 solely to indicate this fact.

PNAS is available online at www.pnas.org.

Abbreviations: NPC, nuclear pore complex; NLS, nuclear localization signal; NES, nuclear export signal; IBB, importin-β-binding domain of importin-α; βGal, β-galactosidase; LMB, leptomycin B.

*To whom reprint requests should be addressed. E-mail: karsten_weis@ls.berkeley.edu.

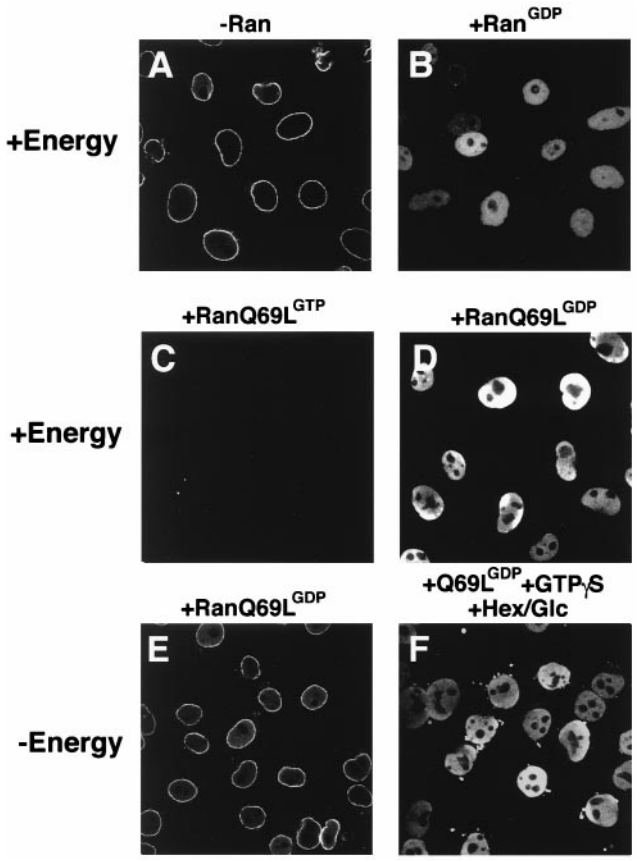

FIG. 1. RanQ69L supports import *in vitro*. Nuclear import of fluorescein-labeled IBB-βGal was assayed in permeabilized cells for 30 min in the presence of 1 μM importin β and buffer alone (*A*), 2.5 μM Ran-GDP (*B*), 2.5 μM RanQ69L-GTP (*C*), or 2.5 μM RanQ69L-GDP (*D–F*). An energy-regenerating system was present in the reactions shown in *A–D*. In the reaction shown in *F*, GTPγS was added to a final concentration of 2.5 mM, and an energy-depleting system was present during the reaction in the form of 0.4 units/μl hexokinase and 10 mM glucose (Hex/Glc). To ensure that no nucleotide triphosphates were present at the beginning of the import reactions, permeabilized cells were also pretreated with hexokinase and glucose before the import reactions in the experiments shown in *E* and *F*. Note that the energy-regeneration system used in *D* could be replaced by 2.5 mM GTP without any decrease in import activity (not shown). The addition of hexokinase/glucose to such a reaction completely abolishes import (not shown), thus showing that this system efficiently depletes GTP in digitonin-permeabilized. The final concentration of the fluorescent import substrate IBB-βGal was 800 nM. Nuclei were scanned with a confocal fluorescence microscope (63× oil objective).

identical settings were used to acquire the data shown in the same panel.

For real-time experiments, 1 μg/ml 4′,6-diamidino-2-phenylindole (Boehringer Mannheim) was included in the wash after permeabilization, and coverslips were inverted onto 6.5 μl of the reaction mixture. Cells were brought into focus by using the UV channel, and fields were scanned no more than once in the FITC channel to avoid photobleaching.

Quantitation of fluorescence was performed on five randomly chosen fields as follows. A rectangular area was selected inside each nucleus while carefully avoiding the nucleolar zone. The average fluorescence intensity was obtained through the HISTOGRAM function in ADOBE PHOTOSHOP 4.0. Between 50 and 100 cells were counted for each experimental point. In the case of the time course, the background was taken equal to an extracellular area, whereas intact cells were used to estimate the background in the real-time experiment. The standard error shown corresponds to the field-to-field variability.

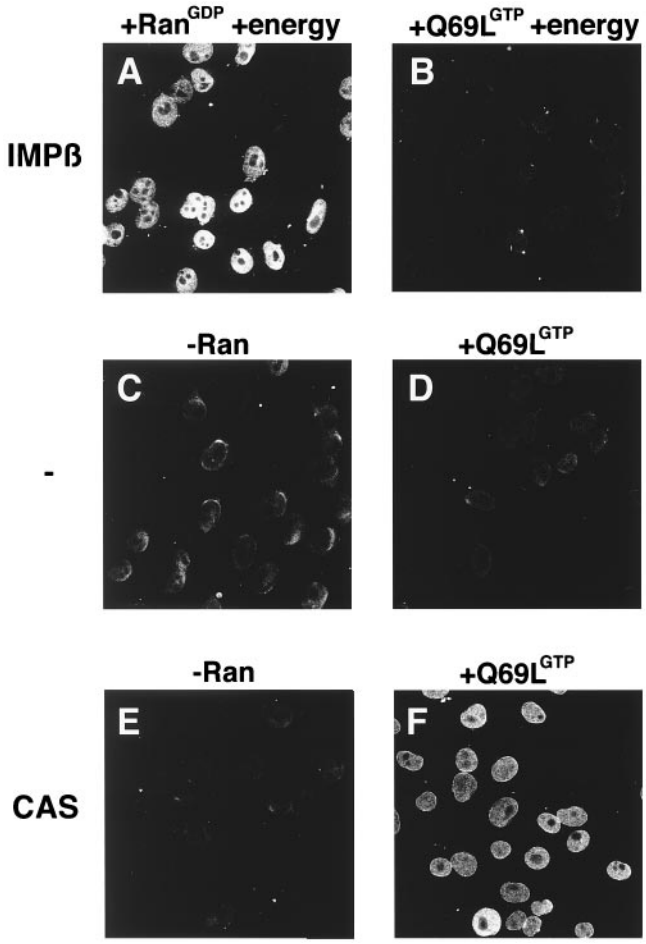

FIG. 2. Importin α is translocated into the nucleus in the presence of CAS and Ran-GTP. Nuclear transport of importin α was assayed in digitonin-permeabilized cells for 30 min at 22°C in the presence of recombinant transport factors. A preformed importin α·β complex was mixed with either Ran-GDP (*A*) or RanQ69L-GTP (*B*) in the presence of an energy-regeneration system before addition to the cells. Similarly, importin α was mixed with buffer alone (*C*), RanQ69L-GTP alone (*D*), CAS alone (*E*), or CAS and RanQ69L-GTP (*F*). Before addition to the cells, mixes were incubated on ice for 3 min to allow for complex formation. ATP, GTP, and an energy-regeneration system were not added in reactions *C–F*. Cells were fixed immediately with paraformaldehyde, and importin α was detected by secondary immunofluorescence (35). The following final concentrations of factors were used in these assays: 1 μM importin α, 1 μM importin β, 2 μM CAS, and 2.5 μM Ran. Nuclei were scanned with a confocal fluorescence microscope (63× oil objective).

RESULTS AND DISCUSSION

Import of NLS-Containing Proteins Does Not Require GTP Hydrolysis. Recently, it was shown that GTP hydrolysis by Ran is not required for the translocation of transport substrates through the NPC (21, 24, 25). To confirm these results, we wanted to test the effects of the mutant Ran protein RanQ69L in the *in vitro* transport assay. RanQ69L cannot efficiently hydrolyze GTP and is insensitive to the action of the Ran-GAP (26). As previously shown (19, 27), recombinant importin-β alone, in the absence of Ran, mediates docking of IBB-βGal (a fusion of IBB to βGal) at the nuclear envelope of digitonin-permeabilized cells (ref. 23; Fig. 1*A*). In the presence of an energy-regeneration system, addition of wild-type Ran-GDP to the import reaction causes efficient translocation of IBB-βGal (Fig. 1*B*). Neither import nor docking was observed when Ran-GDP was replaced with RanQ69L-GTP (Fig. 1*C*), presumably because Ran in its GTP-form dissociates the importin

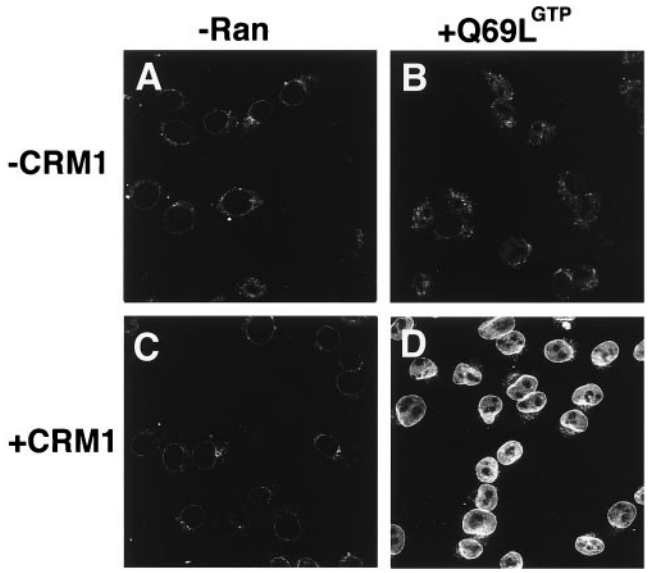

FIG. 3. BSA-NES is translocated into the nucleus in the presence of CRM1 and Ran-GTP. Fluorescein-labeled BSA-NES was mixed with buffer alone (*A*), RanQ69L-GTP alone (*B*), CRM1 alone (*C*), or CRM1 and RanQ69L-GTP (*D*). Mixes were incubated for 3 min on ice to allow for complex formation before addition to digitonin-permeabilized cells. The transport reactions were allowed to proceed at 22°C for 20 min, at which point the cells were immediately fixed on ice with paraformaldehyde. Reactions were performed in the absence of ATP, GTP, or an energy-regeneration system. The following final concentrations of factors were used in these assays: 2.5 μM RanQ69L-GTP, 2 μM CRM1, and 250 nM BSA-NES. Nuclei were scanned with a confocal fluorescence microscope (63× oil objective).

β·IBB-βGal complex in the cytoplasm (7, 15, 16). However, in the presence of an energy-regeneration system, complete and efficient import of IBB-βGal could be detected when RanQ69L was loaded with GDP (Fig. 1*D*). Furthermore, RanQ69L-GDP supported complete transport when the energy-regeneration system was replaced with the nonhydrolyzable GTP analogue GTPγS, even in the presence of an NTP-depleting system (Fig. 1*F*). In the control without additional energy, RanQ69L-GDP did not support import of the IBB-βGal substrate (Fig. 1*E*).

These data confirm that GTP hydrolysis by neither Ran nor any other GTPase is essential for the complete transport reaction *in vitro* (21, 24, 25). Because cytoplasmic Ran-GTP inhibits import (Fig. 1*C*; see also refs. 15 and 16), these results suggest that Ran-GDP has to be converted to Ran-GTP inside the nucleus. This conversion is most likely achieved by the nuclear Ran guanine-nucleotide exchange factor RCC1.

The Directionality of CAS-Mediated Export of Importin α Can Be Inverted. To examine the role of the NPC in determining the asymmetry of nuclear transport, we tested whether the direction of transport can be affected by inverting the Ran-GTP gradient, i.e., by the addition of high concentrations of RanQ69L-GTP to the cytoplasmic phase of the transport reaction.

First, the localization of the NLS-receptor importin α was analyzed in the digitonin-permeabilized cell assay (ref. 23; Fig. 2). In a standard import reaction (containing importin α, its import receptor importin β, Ran-GDP, and energy), importin α efficiently accumulates in nuclei after a 30-min incubation at room temperature (Fig. 2*A*). As expected, no import of importin α could be detected when Ran-GDP was replaced with RanQ69L-GTP, because Ran in its GTP-bound form dissociates the importin α·β dimer (Fig. 2*B*). Incubation with importin α alone (Fig. 2*C*), importin α plus RanQ69L-GTP (Fig. 2*D*), or importin α together with its exportin CAS (Fig. 2*E*) did not induce import of importin α. However, in the presence of RanQ69L-GTP, CAS, and importin α, significant amounts of importin α were detected inside the nucleus (Fig. 2*F*). Because it has been shown that CAS functions as the nuclear export receptor for importin α (10), these data suggest

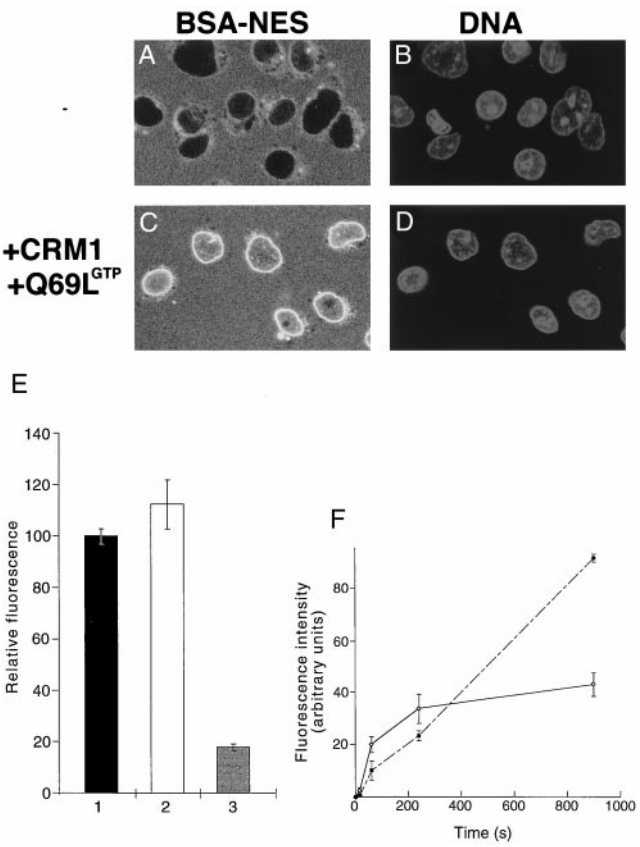

FIG. 4. BSA-NES equilibrates between cytoplasmic and nuclear compartments in the presence of CRM1 and RanQ69L-GTP. Cells grown on coverslips were permeabilized with digitonin and washed in the presence of the DNA-stain 4′,6-diamidino-2-phenylindole. Coverslips were then inverted onto a droplet containing either 250 nM fluorescein-labeled BSA-NES alone (*A* and *B*) or together with 2.5 μM RanQ69L-GTP and 2 μM CRM1 (*C* and *D*). The localization of the fluorescein-labeled BSA-NES was followed by laser scanning confocal microscopy (63× oil objective) through the FITC channel (*A* and *C*), whereas the nuclear DNA was visualized through the UV channel (*B* and *D*). Images were recorded after 10 min of incubation at 22°C. Note that the levels of intranuclear fluorescence in *C* are similar to the level in the surrounding solution, whereas no fluorescent signal can be seen in the nuclei shown in *A*. (*E*) The extracellular fluorescence (bar 1) for the reactions shown in *A* and *C* was compared with the intranuclear fluorescence shown in *C* (bar 2) and with that shown in *A* (bar 3). More than 50 cells from five different fields were analyzed for each data point. The error bars correspond to the standard deviations between fields. (*F*) Kinetics of reversed NES export (solid line) and *Xenopus* extract-driven IBB import (dashed line) were estimated by fixing cells at 15 s, 1 min, 4 min, and 15 min. Use of recombinant factors instead of *Xenopus* extracts for the import of IBB-βGal resulted in a similar, continuous accumulation of substrate over time (data not shown). Because the two substrates differ in the number of conjugated fluorophores, the fluorescence intensities cannot be compared directly between the two assays. To estimate the rate of inverted export, we assumed that the average nuclear diameter is 10 μm (a perfectly round HeLa cell nucleus has therefore a volume of 12.5 pl), that a HeLa cell nucleus contains ≈3,000 NPCs, that at short time points no reexit of the substrate has occurred, and that, at equilibrium, the substrate concentration inside and outside the nuclei was 0.3 μM. Because, at 2 min, the intranuclear intensity is about 50% of that at equilibration, the number of molecules of fluorescein-coupled BSA-NES inside one nucleus is $0.5 \times (0.3 \times 10^{-6}) \times (6 \times 10^{23}) \times (12.5 \times 10^{-12}) = 2.3 \times 10^{6}$, and the number of nuclear entry events per NPC per second is $2.3 \times 10^{6}/(3{,}000 \times 120) = \approx 3.5$.

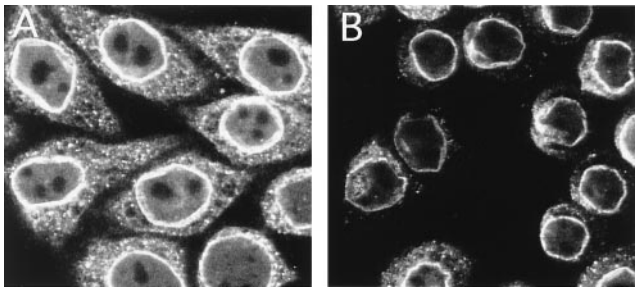

FIG. 5. The imported BSA-NES can be reexported. Reexport of fluorescein-conjugated BSA-NES was assayed in permeabilized cells by loading nuclei for 15 min by using the inverted-export assay as described for Fig. 3, followed by immediate fixation (*A*); alternatively, cells were washed, incubated for an additional 15 min at room temperature in the presence of 2 μM CRM1 and 2.5 μM RanQ69L-GTP, and then fixed (*B*). Nuclei were scanned with a confocal fluorescence microscope (63× oil objective).

that the directionality of importin α export can be inverted *in vitro*.

Inversion of CRM1-Mediated NES Protein Export. The surprising effect of cytoplasmic Ran-GTP on the direction of transport prompted us to investigate the second well characterized nuclear protein export pathway, the export of leucine-rich NES-containing proteins mediated by CRM1/exportin1 (refs. 9, 14, 28, and 29; Fig. 3). As expected, a fluorescently labeled BSA-NES conjugate alone is excluded from the nuclei of digitonin-permeabilized cells (Fig. 3*A*). Neither RanQ69L-GTP alone (Fig. 3*B*) nor CRM1 alone (Fig. 3*C*) caused translocation of BSA-NES through the NPC. In contrast, the addition of CRM1 together with RanQ69L-GTP caused specific uptake of the fluorescent BSA-NES substrate into the nucleoplasm (Fig. 3*D*). From this result, we conclude that the inversion of the Ran-GTP gradient reverses the direction of transport mediated by the exportins CAS and CRM1.

We note that the relative import levels in the inverted transport reactions shown in Figs. 2 and 3 are clearly lower than the respective levels obtained in conventional import reactions. However, because BSA-NES is not retained inside nuclei (22) and RanQ69L cannot hydrolyze GTP to cause complex dissociation inside the nucleus, the second law of thermodynamics would predict that no nuclear accumulation of transport substrates above cytoplasmic levels should be achieved here. In addition, reexport of the BSA-NES·CRM1·Ran-GTP complex can occur readily in these assay conditions (see Fig. 5 and also ref. 21). To test whether the BSA-NES substrate equilibrates between the cytoplasmic and nuclear compartments, transport reactions were performed in the presence of CRM1 and RanQ69L-GTP, and substrate uptake was followed by confocal microscopy in unfixed cells (Fig. 4*C*). Corresponding nuclei were visualized with the DNA-stain 4′,6-diamidino-2-phenylindole (Fig. 4*D*). Quantitation of the transport reaction shown in Fig. 4*C* indicates that BSA-NES equilibrates between the nucleus and the cytoplasm. Although significant amounts of BSA-NES substrate entered the nucleus, no nucleoplasmic accumulation above cytoplasmic levels could be achieved (Fig. 4*E*). In addition to the intranuclear labeling, strong accumulation of the transport substrate at the nuclear periphery was observed (Fig. 3*D*). Because BSA-NES shuttles in this assay (see below), this accumulation may reveal a rate-limiting step during translocation through the NPC. In a control in which CRM1 and Ran-GTP were omitted, BSA-NES is excluded from the nucleus (Fig. 4 *A* and *E*).

To analyze the efficiency and the kinetics of the inverted transport reaction, we performed a time-course experiment and quantitated the amount of nuclear fluorescence for BSA-NES inverted transport (Fig. 4*F*, solid line) and IBB-βGal import (Fig. 4*F*, dashed line). All transport reactions are very rapid, and we estimate ≈3.5 import events per pore per second for the BSA-NES transport (for details see *Methods*). For a comparison, it was calculated that ribosomal protein import occurs at rates of around 2.5 proteins per pore per second *in vivo* (17). However, whereas the amount of NLS substrate in the nucleus increases continuously in the time frame of this experiment, the inverted transport reaction reaches a plateau in less than 5 min.

To test whether both import and export are active in this transport reaction, we performed a chase experiment (Fig. 5). After loading the nuclei for 15 min, cells were fixed and visualized immediately (Fig. 5*A*); alternatively, the buffer was changed, and the intranuclear fluorescence was analyzed after an additional 15-min incubation (Fig. 5*B*). After 15 min, the intranuclear fluorescence decreased to background levels, indicating that export of BSA-NES had occurred.

From these experiments, we conclude that the translocation of BSA-NES into nuclei is a facilitated transport mechanism that leads to the equilibration of the substrate between the cytoplasm and the nucleus but does not cause import against a concentration gradient. Equilibration is presumably accomplished by a very fast shuttling of CRM1·Ran-GTP·BSA-NES complexes between the two compartments without consumption of energy.

The Inverted Import Reaction Mediated by CRM1 Is Blocked by Known Inhibitors of NES-Protein Export. To characterize the inverted transport further, reactions were performed in the presence of well characterized inhibitors of

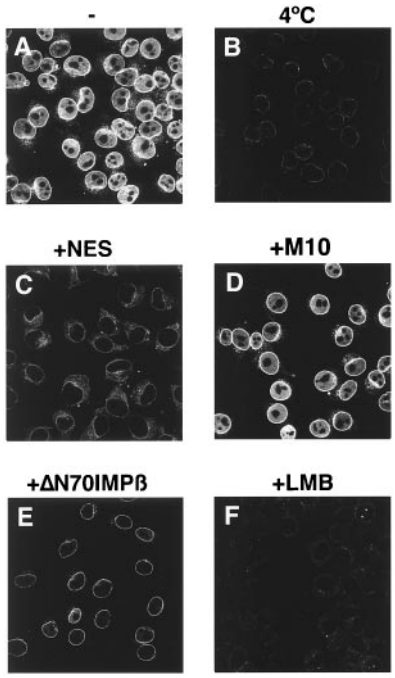

FIG. 6. The import of BSA-NES is sensitive to inhibitors of NES-mediated protein export. Fluorescein-labeled BSA-NES was mixed on ice with the recombinant factors CRM1 and RanQ69L-GTP and added to digitonin-permeabilized cells. In the reaction shown in *C*, a 200-fold molar excess of NES peptide was added. In *D*, the same concentration of the mutant M10 peptide was used instead. (*E*) Import cells were preincubated for 5 min with 4 μM of importin β^{71-876} and washed before addition of the reaction mix. In *F*, leptomycin B (LMB) was added to a final concentration of 10 μM. This concentration of LMB does not affect nuclear import of BSA-NLS in *Xenopus* extracts (data not shown). Nuclear transport assays were allowed to proceed for 20 min at either 22°C (*A* and *C–F*) or on ice (*B*), and cells were fixed immediately with paraformaldehyde. Final concentrations of factors were 2.5 μM RanQ69L-GTP, 2 μM CRM1, and 250 nM BSA-NES. Nuclei were scanned with a confocal fluorescence microscope (63× oil objective).

NES-mediated protein export. When transport reactions were carried out at 4°C, no nuclear uptake could be observed (Fig. 6*B*), excluding a transport mechanism based on free diffusion. Because RanQ69L cannot hydrolyze GTP (26) and no additional NTP hydrolysis is involved here, this temperature sensitivity may reflect the requirement for a conformational change in either the lipid or proteinaceous phase of the NPC. Next, transport assays were performed after preincubation of import cells with the importin β mutant importin β^{71-876} (20). This mutant can no longer bind Ran and has been shown to be a very potent inhibitor of almost all tested import and export pathways (20, 30). Fig. 6*E* shows that BSA-NES import can be inhibited efficiently by importin β^{71-876}, indicating that there is at least one common intermediate between the inverted transport and the importin β-mediated import. BSA-NES transport was also blocked in the presence of a 200-fold molar excess of NES peptide (Fig. 6*C*). In contrast, the same amount of the M10 control peptide did not have any inhibitory effect (Fig. 6*D*). Finally, we also wanted to examine the effects of the export inhibitor LMB (31). LMB specifically inhibits the interaction of CRM1 with NES-containing substrates through direct binding to CRM1 (9). LMB completely abolished nuclear translocation of BSA-NES in this *in vitro* transport reaction (Fig. 6*F*). It can be concluded that the CRM1·RanQ69L-GTP-dependent translocation of BSA-NES into nuclei is specific and can be blocked by the same inhibitors previously shown to block NES-mediated protein export *in vivo*.

A Model for the Translocation Reaction Through the NPC. Structural studies have shown that the NPC has an asymmetric organization with distinct substructures on the nuclear and cytoplasmic side of the complex (1). The data presented here raise the question whether this asymmetry plays an essential role to ensure vectorial transport between the cytoplasm and the nucleus. Using a well characterized *in vitro* transport assay, we show that the directionality of transport through the NPC can be inverted in the presence of high cytoplasmic concentrations of Ran-GTP. This result indicates that the NPC does not provide an intrinsic barrier to reversing the direction of transport by export factors *in vitro*. Because it has been shown that importin β-like transport factors are able to interact with several components of the NPC (7, 32) and to passage through the pore in the absence of other factors or GTP hydrolysis (33, 34), we propose that the NPC has evolved as a highly specialized transporter that selectively allows facilitated and bidirectional transport of cargoes bound to importin β-like import or export receptors (Fig. 7). The translocation of receptor–cargo complexes through the nuclear pore could be achieved by multiple, reversible interactions between nuclear pore proteins and receptors. Although no directionality would be built into these saltatory binding reactions, the vectorial nature of transport would be ensured by an irreversible and energetically favorable last step. For protein import, the final step would be the Ran-GTP-induced dissociation of importin–cargo complexes (7, 8), whereas protein export would be terminated by RanBP1/RanGAP-stimulated GTP hydrolysis by Ran, which causes release of the export substrate into the cytoplasm (10, 11). The hydrolysis of GTP in the cytoplasm would ultimately provide the required energy to create order and to achieve uphill accumulation of substrates.

Obvious open questions in this model are how the NPC achieves its high selectivity and how gating of large substrates

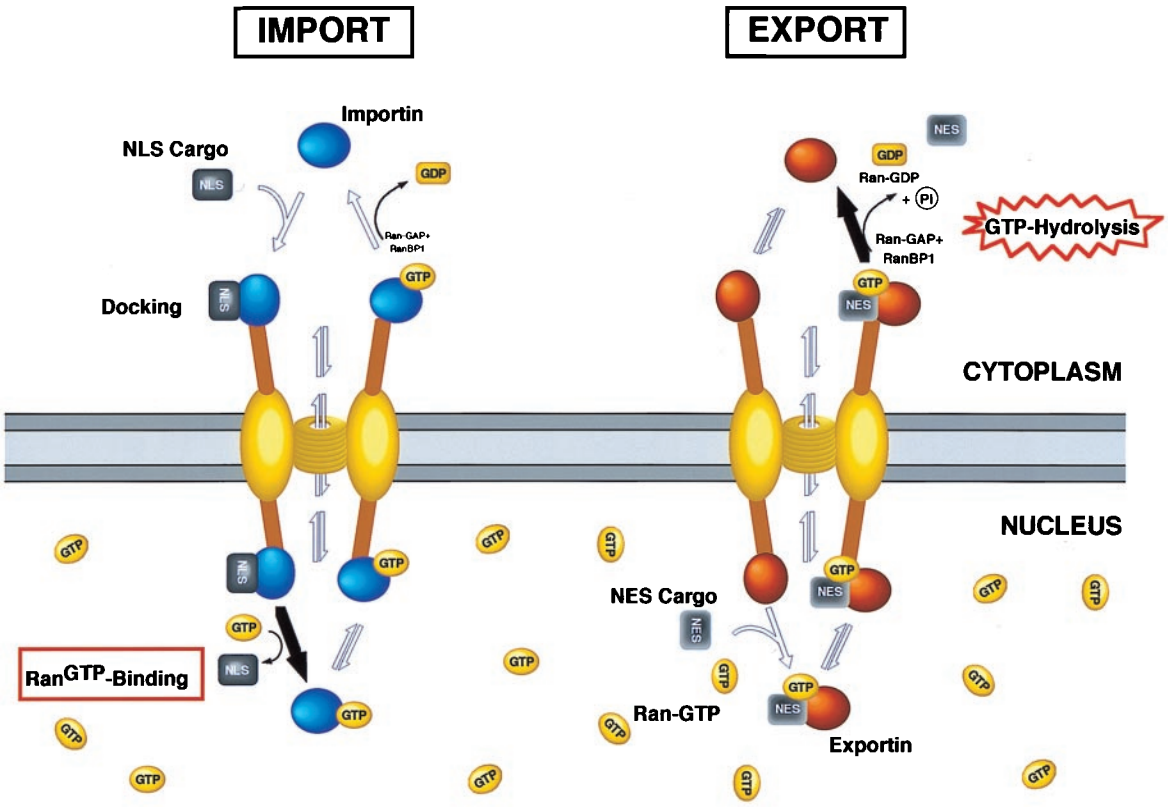

FIG. 7. A model for nucleocytoplasmic transport. In this model, the translocation through the pore involves multiple, reversible interactions between the receptor–cargo complex and proteins of the NPC. No directionality is built into these reactions, but the vectoriality is ensured by a Ran-regulated irreversible last step. Although no consumption of high-energy phosphates is needed for translocation through the pore, the energy potential for import comes from the high nuclear Ran-GTP concentration, whereas export is coupled directly to the RanGAP/RanBP1 induced GTP hydrolysis in the cytoplasm. By the addition of cytoplasmic Ran-GTP, the Ran gradient is inverted, and nuclear translocation of export substrates can occur. Such a model is akin to transport mechanisms of ions through membranes where electrochemical gradients are used to pump ions against their concentration gradient (for details, see *Results and Discussion*).

can be accomplished. The transport reactions studied in this report represent simple nucleocytoplasmic transport processes involving single cargo–receptor interactions. It is to be expected that for more complex transport pathways, such as mRNA export, additional factors are required to ensure proper and directional targeting. Nevertheless, the inverted transport assay presented here reveals important principles about the translocation reaction through the nuclear pore, and it will be interesting to test whether this assay will provide a more general tool to study complex nuclear export events.

We thank the following people for providing plasmids and reagents: L. Englmeier and I. Mattaj for the human CRM1 expression plasmid, U. Brinkmann and I. Pastan for the human CAS clone, D. Lafontaine and D. Tollervey for the pTL27-ZZ vector, D. Görlich for pZZ-Ran and pZZ-RanQ69L clones, S. Adam for importin β and importin β^{71-876} plasmids, J. Morrison for the His-ZZ-Ran clone, R. Heald for *Xenopus* extracts, and B. Wolff and the Novartis Forschungsinstitut for LMB. We are grateful to M. Redd and members of the O'Shea and Guthrie lab for stimulating discussions and to E. O'Shea, P. Walter, A. Lamond, A. Murray, D. Morgan, M. Redd, K. Reif, and A. Kaffman for their comments on the manuscript. M.V.N. was supported by a predoctoral fellowship from the Boehringer Ingelheim Fonds.

1. Panté, N. & Aebi, U. (1996) *Crit. Rev. Biochem. Mol. Biol.* **31,** 153–199.
2. Nigg, E. A. (1997) *Nature (London)* **386,** 779–787.
3. Mattaj, I. W. & Englmeier, L. (1998) *Annu. Rev. Biochem.* **67,** 265–306.
4. Weis, K. (1998) *Trends Biochem. Sci.* **23,** 185–189.
5. Bischoff, F. R. & Ponstingl, H. (1991) *Nature (London)* **354,** 80–82.
6. Bischoff, F. R., Klebe, C., Kretschmer, J., Wittinghofer, A. & Ponstingl, H. (1994) *Proc. Natl. Acad. Sci. USA* **91,** 2587–2591.
7. Rexach, M. & Blobel, G. (1995) *Cell* **83,** 683–692.
8. Izaurralde, E., Kutay, U., von Kobbe, C., Mattaj, I. W. & Görlich, D. (1997) *EMBO J.* **16,** 6535–6547.
9. Fornerod, M., Ohno, M., Yoshida, M. & Mattaj, I. W. (1997) *Cell* **90,** 1051–1060.
10. Kutay, U., Bischoff, F. R., Kostka, S., Kraft, R. & Görlich, D. (1997) *Cell* **90,** 1061–1071.
11. Kutay, U., Lipowsky, G., Izaurralde, E., Bischoff, F. R., Schwarzmaier, P., Hartmann, E. & Görlich, D. (1998) *Mol. Cell* **1,** 1–20.
12. Arts, G. J., Fornerod, M. & Mattaj, I. W. (1998) *Curr. Biol.* **8,** 305–314.
13. Kaffman, A., Rank, N. M., O'Neill, E. M., Huang, L. S. & O'Shea, E. K. (1998) *Nature (London)* **396,** 482–486.
14. Stade, K., Ford, C. F., Guthrie, C. & Weis, K. (1997) *Cell* **90,** 1041–1051.
15. Görlich, D., Panté, N., Kutay, U., Aebi, U. & Bischoff, F. R. (1996) *EMBO J.* **15,** 5584–5594.
16. Weis, K., Dingwall, C. & Lamond, A. I. (1996) *EMBO J.* **15,** 7120–7128.
17. Görlich, D. & Mattaj, I. W. (1996) *Science* **271,** 1513–1518.
18. Richards, S. A., Carey, K. L. & Macara, I. G. (1997) *Science* **276,** 1842–1844.
19. Weis, K., Ryder, U. & Lamond, A. I. (1996) *EMBO J.* **15,** 1818–1825.
20. Chi, N. C. & Adam, S. A. (1997) *Mol. Biol. Cell* **8,** 945–956.
21. Englmeier, L., Olivo, J. C. & Mattaj, I. W. (1999) *Curr. Biol.* **9,** 30–41.
22. Fischer, U., Huber, J., Boelens, W. C., Mattaj, I. W. & Lührmann, R. (1995) *Cell* **82,** 475–483.
23. Adam, S. A., Marr, R. S. & Gerace, L. (1990) *J. Cell Biol.* **111,** 807–816.
24. Schwoebel, E. D., Talcott, B., Cushman, I. & Moore, M. S. (1998) *J. Biol. Chem.* **273,** 35170–35175.
25. Ribbeck, K., Kutay, U., Paraskeva, E. & Görlich, D. (1999) *Curr. Biol.* **9,** 47–50.
26. Klebe, C., Bischoff, F. R., Ponstingl, H. & Wittinghofer, A. (1995) *Biochemistry* **34,** 639–647.
27. Görlich, D., Henklein, P., Laskey, R. A. & Hartmann, E. (1996) *EMBO J.* **15,** 1810–1817.
28. Ossareh-Nazari, B., Bachelerie, F. & Dargemont, C. (1997) *Science* **278,** 141–144.
29. Fukuda, M., Asano, S., Nakamura, T., Adachi, M., Yoshida, M., Yanagida, M. & Nishida, E. (1997) *Nature (London)* **390,** 308–311.
30. Kutay, U., Izaurralde, E., Bischoff, F. R., Mattaj, I. W. & Görlich, D. (1997) *EMBO J.* **16,** 1153–1163.
31. Wolff, B., Sanglier, J. J. & Wang, Y. (1997) *Chem. Biol.* **4,** 139–147.
32. Moroianu, J., Hijikata, M., Blobel, G. & Radu, A. (1995) *Proc. Natl. Acad. Sci. USA* **92,** 6532–6536.
33. Nakielny, S. & Dreyfuss, G. (1997) *Curr. Biol.* **8,** 89–95.
34. Kose, S., Imamoto, N., Tachibana, T., Shimamoto, T. & Yoneda, Y. (1997) *J. Cell Biol.* **139,** 841–849.
35. Nachury, M., Ryder, U. W., Lamond, A. I. & Weis, K. (1998) *Proc. Natl. Acad. Sci. USA* **95,** 582–587.